Endothelial Notch4 signaling induces hallmarks of brain arteriovenous malformations in mice

Patrick A. Murphy*, Michael T. Y. Lam*†, Xiaoqing Wu*‡, Tyson N. Kim*, Shant M. Vartanian*, Andrew W. Bollen§, Timothy R. Carlson*¶, and Rong A. Wang*∥

*Pacific Vascular Research Laboratory, Division of Vascular Surgery, Department of Surgery, and Department of Anatomy and §Department of Pathology, University of California, San Francisco, CA 94143

Brain arteriovenous malformations (BAVMs) can cause devastating stroke in young people and contribute to half of all hemorrhagic stroke in children. Unfortunately, the pathogenesis of BAVMs is unknown. In this article we show that activation of Notch signaling in the endothelium during brain development causes BAVM in mice. We turned on constitutively active Notch4 (*int3*) expression in endothelial cells from birth by using the tetracycline-regulatable system. All mutants developed hallmarks of BAVMs, including cerebral arteriovenous shunting and vessel enlargement, by 3 weeks of age and died by 5 weeks of age. Twenty-five percent of the mutants showed signs of neurological dysfunction, including ataxia and seizure. Affected mice exhibited hemorrhage and neuronal cell death within the cerebral cortex and cerebellum. Strikingly, *int3* repression resolved ataxia and reversed the disease progression, demonstrating that *int3* is not only sufficient to induce, but also required to sustain the disease. We show that *int3* expression results in widespread enlargement of the microvasculature, which coincided with a reduction in capillary density, linking vessel enlargement to Notch's known function of inhibiting vessel sprouting. Our data suggest that the Notch pathway is a molecular regulator of BAVM pathogenesis in mice, and offer hope that their regression might be possible by targeting the causal molecular lesion.

angiogenesis | cell signaling | endothelial cell | stroke | cerebrovascular

Approximately 600,000 people worldwide harbor brain arteriovenous malformations (BAVMs) that can potentially rupture, leading to stroke and death. Historically, 50% of BAVMs first present with hemorrhage (1). Development of noninvasive imaging methods has increased BAVM detection before hemorrhage, but the efficacy of current treatments, primarily surgical resection, is questionable. Accompanying risk of mortality (3%) and morbidity (9%) may outweigh the risk of rupture itself (2). An ongoing clinical trial (ARUBA) is testing the hypothesis that invasive treatment may not provide a significant improvement over the natural course of the disease (2).

BAVMs disrupt normal vessel hierarchy and are caused by the replacement of capillary beds, which separate arteries from veins, with enlarged and tangled vessels. The retention of characteristics of embryonic brain vasculature in BAVMs has led to the speculation that they form during early brain development (3). Studies of a more accessible skin arteriovenous malformation (AVM) in human beings suggests that enlargement of postcapillary venules precedes AVM formation (4), but experimental evidence is required to validate such mechanisms. An animal model that mimics the characteristics of human BAVMs, principally arteriovenous shunting, would open avenues to understanding their cellular and molecular pathogenesis.

The primary factors regulating vessel hierarchy were once thought to be hemodynamic forces (5). It is now known that genetic programs contribute to the development of vascular hierarchy by specifying arteries and veins (6). Notch signaling has emerged as a critical genetic mediator in the differentiation of arteries and veins. Originally discovered in *Drosophila*, the transmembrane Notch receptor is conserved throughout the animal kingdom and is best known for its function in dichotomous cell fate decisions through cell–cell communication (7). Ligand binding to its extracellular domain results in sequential cleavage events and release of an active intracellular domain (ICD), which then translocates to the nucleus and initiates transcription of downstream genes (7). Thus, nuclear localization of Notch-ICD is a hallmark of Notch activation.

In the vascular system, Notch receptors and ligands are expressed in arteries but not veins (8) and are necessary and sufficient to induce ephrin-B2, a faithful marker of arterial identity (9–11). Notch loss-of-function mutations impair vascular development, resulting in arteriovenous shunting in both zebrafish and mouse embryos (10, 12). Notch gain-of-function also results in abnormal vascular remodeling in embryos, demonstrating that proper spatial and temporal patterns of Notch activity are critical for this process (13). Because BAVMs are thought to occur during brain development (3), we hypothesized that expression of constitutively active Notch4 would induce BAVMs during the neonatal period, when areas of the brain, such as the neocortex and cerebellum, expand by nearly 10-fold (14).

Results

Expression of Constitutively Active Notch4 (int3) in the Endothelium Results in Hemorrhage, Neurological Damage, and Death in Neonates. To test our hypothesis that Notch4 activation in the endothelium of the developing brain would cause BAVM, we expressed int3 specifically in the endothelium from birth in tetracycline-regulated mice (*Tie2-tTA;TRE-int3*) (11). Endothelial-specific expression was demonstrated by a *TRE-LacZ* reporter (11, 15) [supporting information (SI) Fig. S1]. In addition, Notch4-ICD was detected in the nuclei of a subset of mutant but not control endothelial cells (ECs) (Fig. 1*A* and *B*). Because int3 is a portion of Notch4, the anti-Notch4-ICD staining could not distinguish int3 from endogenous Notch4. However, the staining did not detect endogenous levels of Notch4 in the control, suggesting that staining in the mutant represents int3 expression. The nuclear accumulation of Notch4-ICD indicates increased Notch4 activity specifically in ECs of mutant mice.
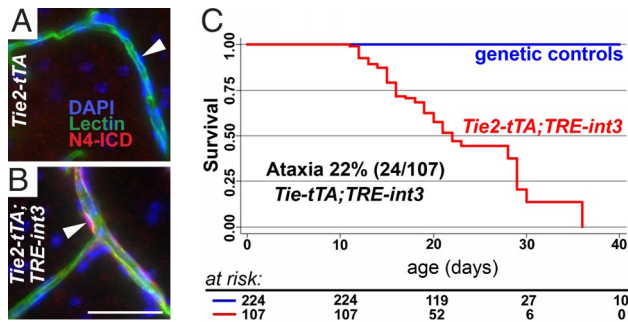
MEDICAL SCIENCES

Fig. 1. Endothelial expression of *int3* causes ataxia and death in neonatal mice. (*A* and *B*) Increased Notch4 activation specifically in the ECs lining lectin-perfused vessels of P29 mutant brain was revealed by nuclear staining of Notch4 intracellular domain (N4-ICD). DAPI-labeled EC nuclei (white arrowheads). (*C*) Kaplan–Meier survival curve shows that all mutants died by P36. (Scale bar, 50 μm.)

Mutant mice died between 2 and 5 weeks of age (Fig. 1*C*). Signs of neurological dysfunction, including ataxia and seizure, were evident in 27 of 107 mutant mice. Ataxia ranged in severity, from mice unable to right themselves to those with splayed rear legs. We occasionally noticed seizure episodes in which the mice ran wildly before collapsing. All but one of the cases of ataxia (23/24) and seizure (5/6) occurred before P22, suggesting that younger mice are more susceptible to these phenotypes.

To investigate potential causes for the neurological dysfunction, we examined mutant brains and found prominent hemorrhage by gross inspection (Fig. 2*B*) and by histology (Fig. 2 *C–F*). Hemorrhage occurred most often in the cerebellum, followed by the neocortex, but never in brainstem. We examined six of the ataxic mice and found hemorrhage in the cerebellum (see Fig. 2 *C* and *D*). Hemorrhage appeared more widespread than the neurological phenotype, because we also observed hemorrhage in all ill mutant mice without detectable ataxia (13 of 13; see Fig.
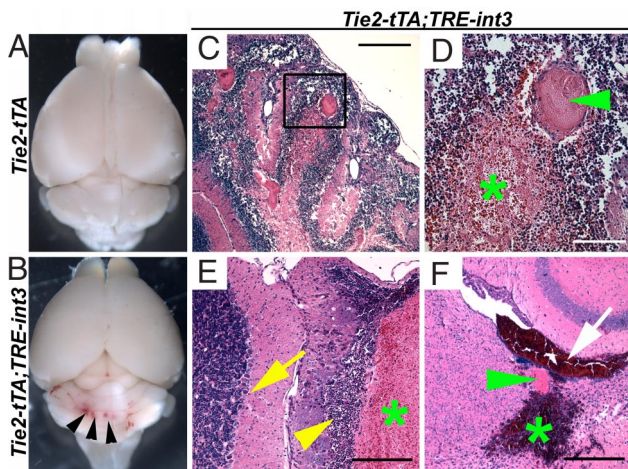

Fig. 2. Brain hemorrhage occurred in all mutant mice. (*A* and *B*) Multifocal hemorrhage (arrowheads) revealed in mutants after vascular perfusion. (*C* and *D*) H&E stained sagittal sections of perfusion fixed cerebellum from a mutant with ataxia show hemorrhage (green asterisk) and thrombosis (green arrowhead). (*E*) H&E stained sagittal section of cerebellar folia from a mutant without ataxia shows hemorrhage (green asterisk) and adjacent dropout of granular and Purkinje neurons (yellow arrowhead). Normal neuronal architecture (yellow arrow) is away from the hemorrhage. (*F*) H&E stained axial section of a severely affected mutant shows intraventricular hemorrhage (white arrow) immediately adjacent to a large, thrombosed vessel (green arrowhead) and parenchymal hemorrhage (green asterisk) in the cerebrum. (Scale bars: *C* and *F*, 400 μm; *D*, 100 μm; *E*, 200 μm.)
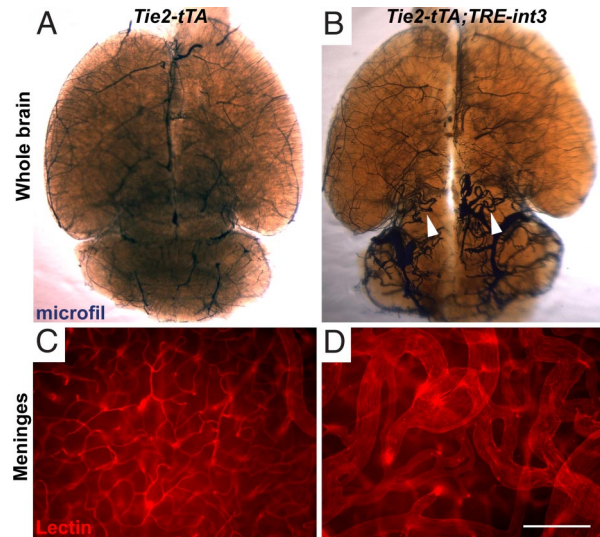

Fig. 3. Enlarged and tangled blood vessels developed in all mutant mice. Vessel enlargement occurred within the parenchyma and on the surface of the brain. Large tangled vessels were shown in the parenchyma of the cerebellum and midbrain by vascular casting at P27 (*B*; white arrowheads) and in the lateral meninges by whole mount imaging of Cy3-labeled lectin perfusion (*D*). (*A* and *C*) Abnormal vessels were not observed in littermate controls. (Scale bar, 200 μm.)

2*E*) and none in their littermate controls. Thrombosis, often a consequence of hemorrhage (16), was seen in hemorrhagic areas (see Fig. 2 *D* and *F*). As with the neurological phenotype, hemorrhage was most severe in mice ill before P22. Blood was found in the ventricle of 4 of 11 ill mice before P21 (see Fig. 2*F*). Neuronal cell death consistently occurred adjacent to hemorrhage (see Fig. 2*E*), suggesting that hemorrhage led to neuronal damage. Foci of pyknotic and karyorectic nuclei, often associated with macrophage infiltrations, were detected in the Purkinje and granular layers of the cerebellum, as well as areas of the neocortex and midbrain (see Fig. 2*E*). Signs of calcification, an indication of earlier cerebral damage, occurred in multiple cases (data not shown). Therefore, increased endothelial Notch4 activation results in hemorrhage, which likely causes neuronal damage and ataxia in the mutant mice.

Vessel Enlargement and Hallmarks of BAVMs in Mutants Before Hemorrhage. Because increased Notch4 activation was targeted to ECs specifically, we investigated lesions underlying hemorrhage and found vascular abnormalities resembling BAVMs. Vascular perfusion with casting agents (Fig. 3*B*) or fluorescent lectins (Fig. 3*D* and Fig. S2) revealed enlarged and tangled vessels, hallmarks of BAVMs (1, 17). We verified that arteries, veins, and intervening vessels were all enlarged, by examining the arterial and venous branches of the middle-cerebral vessels (see Fig. S2). To determine whether the enlarged vessels had smooth muscle coverage, we performed immunofluorescence with anti-smooth muscle α-actin (SMA) and found strong staining in these vessels (Fig. S3). Vessel enlargement occurred before hemorrhage, neuronal cell death, or signs of neurological dysfunction (Fig. S4), suggesting that it is a primary defect.

Because hemorrhage occurred primarily in the cerebellum, followed by the neocortex, and never in brainstem, we tested whether vessel enlargement correlated with hemorrhage. A decrease in the proportion of small vessels and an increase in the proportion of larger vessels were most significant in the cerebellum, followed by the neocortex, and least in brainstem (Fig. 4). Therefore, regional enlargement correlated with hemor-
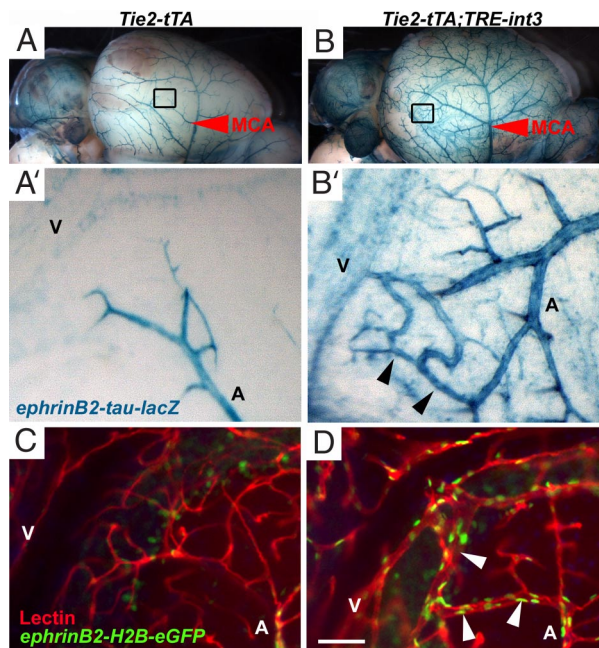
Fig. 4. Increased vessel size and decreased vessel density correlated with the frequency of hemorrhage. Shown is immunofluorescence in sagittal sections of brain regions. Density graphs represent FITC-lectin perfused (red) and total CD31 immunostained (black) vessels in each region (per squared millimeter). Δ Proportion of vessel with given diameter represents the percent change in the proportion of small (<7.5 μm), medium (7.5–20 μm), and large (>20 μm) diameter vessels in each region, relative to average controls. (*A* and *B*) *Tie2-tTA* (n = 6) and *Tie2-tTA;TRE-int3* (n = 3); (*C, D, E,* and *F*), *Tie2-tTA* (n = 6) and *Tie2-tTA;TRE-int3* (n = 5). Values represent mean ± SEM. (Scale bars, 200 μm.)

rhage, supporting the hypothesis that vessel enlargement contributes to hemorrhage.

Endothelial Notch activity decreases vessel density by inhibiting sprouting angiogenesis (18). To investigate vessel density, we quantified CD31 positive vessels. Vessel density was decreased significantly in the cerebellum, and progressively less so in the neocortex and brainstem (see Fig. 4). Vessel density was inversely correlated with the proportion of large vessels (>50 μm) across all of these regions (Fig. S5), suggesting that vessel enlargement is linked to the reduction in vessel density.

Arteriovenous Shunting Occurs in all Mutants. The fundamental defect in human BAVMs is high-flow arteriovenous shunting. Blood velocity in carotid arteries can double in BAVM patients, a clinical indication of arteriovenous shunting (19). We measured carotid blood velocity with high-resolution ultrasound and found increased carotid blood velocity in all mutants by 3 weeks of age (Fig. 5A). This noninvasive approach allowed for progressive measurements in the same animal, demonstrating that carotid blood velocity increased in a short time window between

Fig. 5. All mutants developed shunting and arteriovenous malformations. (*A*) Increased carotid blood flow was detected by P21. Maximal (systolic) carotid blood velocity was measured by pulsed-wave Doppler ultrasound. *Tie2-tTA* and *Tie2-tTA;TRE-int3* (n = 9 and n = 6) at P15; (n = 12 and n = 14) at P17; (n = 16 and n = 26) at P21; (n = 18 and n = 12) at P23; (n = 14 and n = 9) at P29; values represent mean ± SEM. Changes were highly significant from P21 (***, $P < 0.00005$). Typical Doppler traces from mice at P21 (*A Right*). (*B*) Brain arteriovenous shunts developed by P19 as shown by fluorescent microsphere passage. The microspheres bypassed the brain and lodged in the lung in the mutants but not controls. BF, Bright-field; FITC, green fluorescent images.

P17 and P21 (see Fig. 5A). Furthermore, at P21, velocity in mutants with neurological dysfunction was significantly higher than those without neurological dysfunction (2.6 ± 0.5 m/sec; n = 6 versus 1.9 ± 0.5 n = 20, respectively; P = 0.007). Because of limitations of this assay, we were unable to examine sick mutants before this age, and they often exhibited severe neurological defects. As a result, the cohort of mice examined did not display severe neurological defects, which may contribute to the minimal increase at P15.

To more directly test for arteriovenous shunts, we performed a microsphere passage assay (11). Microspheres lodged within the control brain (Fig. 5B) but bypassed the mutant brain and lodged in the downstream lung (*Tie2-tTA* n = 6; *Tie2-tTA;TRE-int3* n = 5). This result demonstrates the existence of arteriovenous shunts in the brain, mimicking the principal defect of human BAVMs.

To directly visualize arteriovenous shunts, we distinguished arterial from venous branches with the arterial marker ephrin-B2. Expression of the reporter in *ephrin-B2+/tLacZ* mice (6) was strong in the middle cerebral arteries and weak in the middle cerebral veins (Fig. 6A). In mutants, direct connections between the arteries and veins were prominent at P21 (Fig. 6B). Similar arteriovenous connections within the cerebellum were detected by using a nuclear GFP reporter in *ephrin-B2+/GFP* mice (20). Cerebellar interfolial arteries (GFP+) in the control follow a typical pattern of branching and ramifying into a fine capillary bed within the granular layer before coalescing into the draining veins (GFP−) (Fig. 6C) (21). However, in mutants there were enlarged vascular connections, replacing normal capillaries, between the interfolial arteries and veins (Fig. 6D). Therefore, direct arteriovenous shunts were visible in the surface and deep cerebellar vasculature of mutant mice.

Repression of *int3* Rescues Moribund Mice. Taking advantage of the tetracycline-regulated expression system, we tested whether

Murphy *et al.*

MEDICAL SCIENCES

Fig. 6. Enlarged arteriovenous connections developed on the meningeal surface and in the parenchyma of mutant brains. (*A* and *B*) X-gal staining of *ephrin-B2*$^{+/tLacZ}$ brains revealed the middle cerebral artery (MCA, red arrowheads) on the lateral side of the brain. High magnification image of the boxed area in *B* shows direct arteriovenous connections (black arrowheads) between arterial branches of the MCA (A) and venous vessels (V) in *Tie2-tTA;TRE-int3;ephrin-B2*$^{+/tLacZ}$ mice (*B′*). (*C* and *D*) Fluorescent images of sagittal cerebellar 100-μm thick sections show enlarged connections (white arrowheads) between GFP-labeled interfolial arteries of *Tie2-tTA;TRE-int3;ephrin-B2*$^{+/tLacZ}$ mice (A) and draining veins (V) in the mutant (*D*) and not control (*C*). (Scale bar, 50 μm.)

repression of the causal genetic lesion could reverse disease progression in mutant mice. Vascular enlargement and shunting occurred in all mutant animals by P21, so this time-point was chosen for a regression study. Littermates were allowed to express the *int3* transgene from birth until P20 or P21, at which time sick mutants were fed doxycycline (Dox), a more stable derivative of tetracycline (Tet), to repress *int3* expression. No mutants survived to P32 without Dox treatment (*n* = 19), but 8 of 9 mutants fed Dox appeared outwardly healthy and active at P35, and were healthy until killed by P64 (Fig. 7*A*). The one exception was a severely affected mutant that died in the first day of treatment.

To investigate the reversal of brain abnormalities specifically, we examined the recovery of ataxic mice. Ataxia in all seven mice examined was resolved within just days of transgene repression (Fig. 7*B*). These findings suggest that repression of endothelial *int3* expression, the causal stimulus, recovers brain function in mutant mice.

Discussion

We demonstrate that increased Notch4 activity causes vascular abnormalities with the characteristics of BAVM, implying that increased Notch4 activation is a potential molecular cause of human BAVM. Our findings also suggest that regression of this devastating disease may be possible by targeting the causal molecular lesion. The activated Notch4 model provides a powerful platform for the study of the pathogenesis and regression of BAVM-like lesions. In addition, our studies of pathogenesis in this model provide experimental support for the hypothesis that BAVMs occur in the developing brain and that they can be induced by vessel enlargement.
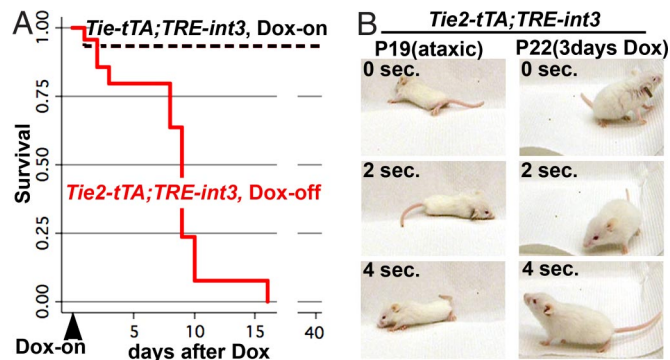

Fig. 7. Repression of *int3* resolved ataxia and prevented death. (*A*) Repression of *int3* with Dox at P20 or P21 allowed the survival of mutant mice, as shown by the Kaplan–Meier curve. *Tie2-tTA;TRE-int3* Dox-off (*n* = 23) and *Tie2-tTA;TRE-int3* Dox-on (*n* = 15) at 20 days; *Tie2-tTA;TRE-int3* Dox-off (*n* = 0) and *Tie2-tTA;TRE-int3* Dox-on (*n* = 5) at 40 days. (*B*) Ataxia was resolved by *int3* repression. Still frames were taken from a movie of a severely ataxic mutant at P19, and upon its recovery at P22, after 3 days of Dox treatment.

Notch4 Activation Is a Candidate in the Molecular Regulation of BAVM Pathogenesis. Molecular etiology of BAVM is unknown. Mutations in the TGF-β signaling pathway, primarily loss-of-function *ENG* (*endoglin*) and *ACVRL1* (*ALK-1*) alleles, have been associated with BAVMs (22). However, these mutations are implicated in only ≈2% of all BAVMs (23). We found that constitutively active Notch4 causes BAVM-like lesions promptly in neonates, identifying activation of the Notch4 pathway as a potent molecular candidate in the development of human BAVMs.

The primary characteristic of human BAVMs is the development of arteriovenous shunting (1). In patients, this is detected by arteriography, the gold standard in the diagnosis of this vascular lesion (24), and also by ultrasound measurement of increased carotid blood flow (25). We demonstrated the presence of arteriovenous shunting by similar methods in mice, including anatomical connections between arteries and veins, functional passage of beads too large for capillaries, and increased carotid blood velocity.

Enlarged and tangled vessels are another key characteristic of BAVMs (1). We detected massively enlarged and tangled vessels by perfusion labeling with a casting agent and fluorescently labeled lectins. In contrast to human BAVMs, which usually develop as a single nidus (23), the vascular abnormalities in mutants were multifocal and widespread. This difference is likely because of the expression of the *int3* transgene throughout the endothelium.

Hemorrhage, often resulting in neuronal damage and ataxia, is the most feared consequence of human BAVM (26). All of the sick mutants examined developed brain hemorrhage, often with adjacent neuronal cell death. Approximately 25% of the mice developed neurological deficits, including ataxia and seizure.

Repression of *int3* Expression Leads to Recovery of Sick Mice. It is commonly thought that natural regression of BAVMs does not occur (27); instead they increase in size and eventually rupture (26). Regression of BAVMs has been reported in only a handful of cases, which are thought to be caused by thrombotic occlusion, a naturally occurring event similar to the embolizing treatments used clinically (27). The recovery of brain function in our mutant mice that resulted from molecular intervention is provocative.

One potential caveat is that Dox, which is used to repress transgene expression, can also inhibit both vessel growth and hemorrhage (28–30), and may therefore contribute to recovery. Because the dose of Dox for transgene repression is similar to

that used for inhibition of vessel growth, we are currently unable to delineate these two effects. However, similar Tet-regulated mouse genetic approaches were used to show that tumors regress after repression of transgenic oncogene expression, inspiring the oncogene addiction theory (31–33). It is possible that Notch4-induced BAVM-like lesions require continuous Notch4 activation for their maintenance.

Regardless whether the Dox-mediated regression is because of repression of transgene expression or because of its direct effect on vessel growth and hemorrhage, the recovery of the ill mice is evocative. Although further studies are required to determine whether this is a result of regression of the BAVM-like lesions, our findings raise the hope that inhibition of the causal molecular lesion may lead to regression of the disease.

High Penetrance and Rapid Onset of BAVM-Like Lesions in the Activated Notch4 Mutants Provide a Robust Platform to Model Human BAVM Pathogenesis. Our transgenic mice provide a much needed mouse model for the study of BAVM pathogenesis. The study of the cellular and molecular etiology of BAVMs is limited by the lack of a good animal model for this disease (34). Mice with mutations in endoglin or ALK-1 have advanced the understanding of molecular contributions to AVMs. Autosomal dominant mutations in these genes are responsible for the human hereditary hemorrhagic telengectasia (HHT) (22), which involves AVMs primarily in the skin, liver and lung, along with a 4% incidence in the brain (35). Of 22 $endoglin^{+/-}$ mice that developed an HHT phenotype, 8 showed signs of brain hemorrhage by $\approx$40 weeks of age (36). Vascular brain casts showed small clusters of capillaries or aneurismal dilations in 3 of 10 $endoglin^{+/-}$ mice (37). Cerebrovascular abnormalities are also observed in $\approx$2% of $Alk-1^{+/-}$ mice (38). However, it is unknown whether either the $endoglin^{+/-}$ or $Alk-1^{+/-}$ mice develop arteriovenous shunting. Therefore, our activated Notch4 mice provide a model for molecular understanding of both the development and potentially the regression of BAVMs.

Notch4 Activity May Selectively Induce BAVM-Like Lesions in Growing Brains. BAVMs typically affect children and younger people. Based primarily on the belief that BAVMs retain embryonic vascular structures, it has been speculated that BAVMs occur during brain growth (26). Our data supports the theory that the growing brain is more vulnerable to BAVM formation. First, we found that hallmarks of BAVM are prominent when the transgene is expressed in the neonatal period, when the brain grows rapidly, but not when it is expressed in the postweaning mouse (11), when brain growth is reduced. Second, we found that vessel enlargement was greatest in the cerebellum and cortex and least in the brainstem, which correlates with the greater growth in the cortex and cerebellum than in the brainstem at this stage (39). Third, when AVMs occur in older mice, they appear to affect the liver, skin, and uterus, three actively remodeling tissues in adult mice (11). These data support the hypothesis that Notch functions in a temporal and spatial specific manner, and that the developing brain is particularly susceptible to Notch4-mediated formation of BAVM-like lesions.

Vessel Enlargement May be a Mechanism for the Onset of BAVMs. The cellular mechanism of BAVM formation is currently unknown. A few models, however, are proposed. The most favored model is that BAVMs represent a failed transition from embryonic brain vasculature to adult brain vasculature (3). Supporting evidence for this theory has rested heavily on the interpretation of the morphological structure of adult BAVMs. Another theory is that BAVMs are not necessarily congenital abnormalities, but can form *de novo* through vessel enlargement. This theory is based on the observation that enlargement of postcapillary venules is the first observable phenotype in the development of AVMs in human skin (4).

Our data support the theory of *de novo* formation of BAVMs through vessel enlargement in the context of growing brain. We are able to measure carotid blood flow, a sensitive indicator of brain arteriovenous shunting, longitudinally in our mutant mice. By this measurement, we were able to show that in individual mutant mice, there was no shunting at P15, but that shunting increased dramatically over the subsequent 6-day period. In addition, the diameters of all vessels, including those at the capillary level, were enlarged. The enlargement of vessels before brain hemorrhage or neurological phenotypes suggests that it plays a causal role in the development of BAVM-like lesions. Thus, our data support the hypothesis that vessel enlargement promotes the development of BAVMs.

An alternative possibility is that Notch activation disrupts the arteriovenous interface by increasing arterial specification. We and others have shown that Notch activity promotes arterial specification in ECs *in vivo* in embryonic and adult mice, as determined by the expression of arterial markers, such as ephrin-B2 (9–11). In this study we found that in neonatal brain endothelium, Notch4 activity increased ephrin-B2 expression in capillaries and veins. Interestingly, expression was most markedly increased in direct arteriovenous connections, suggesting that induction of arterial specification in these ECs may disrupt the proper formation of the capillary bed connecting the artery and vein.

Notch Activity May Promote Vessel Enlargement by Inhibiting Sprouting. We previously reported that Notch activity promotes vessel enlargement (11), and others subsequently demonstrated a reduction in vessel density (18), but the relationship of these functions is unclear. We observed a correlation between vessel enlargement and vessel density, suggesting that Notch's role in decreasing vessel density might be intimately involved with vessel enlargement and BAVM development. Supporting our finding, it was recently reported that retroviral expression of the Notch ligand Dll4 increases lumen diameters and reduces vessel density in grafted tumors in mice (40). The observation that impaired endothelial sprouting can result in vessel enlargement was first made in mice exclusively expressing the $VEGF_{120}$ isoform (41). In both the VEGF mutant and our previous studies (11), proliferation was not significantly altered, suggesting that increased vessel size may simply reflect the retention of cells that would have otherwise contributed to sprouts. Therefore, Notch activation may promote vessel enlargement by inhibiting vessel sprouting.

In summary, we believe that this work opens an area of research to advance the molecular understanding of BAVM pathogenesis and provides hope for the treatment of this devastating disease.

Methods

Mice. Tet sucrose solution (0.5-mg/ml Tet, 50-mg/ml sucrose, Sigma) was administered to pregnant mothers from plugging, and withdrawn from pups at birth, and Dox (200-mg/kg diet, Bio-Serv) diet was administered to mutant mice at P20–21 as we described (11, 42). All animals were treated in accordance with the guidelines of the University of California San Francisco Institutional Animal Care and Use Committee.

Vascular Imaging. β-gal was detected by activity or with an anti-β-gal antibody as we described (11). Casting and FITC-lectin staining were performed as we described (11). Cy3-streptavidin (Jackson Immuno) was used to detect biotinylated lectin (Vector Labs); these reagents were coinjected into circulation (25 μg of each in 200-μl PBS). Immunostaining was performed with anti-CD31, anti-α-SMA, and anti-Notch4 (Upstate) according to our published protocols (43, 44).

Statistical Analysis. All values represent the mean ± SEM. Kaplan–Meier survival curves were generated with STATA-IC software. See *SI Methods* for density and diameter analysis.

Vascular Shunting. Fifteen-μm fluorescent microspheres (Molecular Probes) were injected into the left carotid artery of anesthetized mice, and tissues were examined with a fluorescence dissecting microscope. For ultrasound measurements of carotid velocity, mice were anesthetized with isoflurane and body temperature was maintained on a heat pad. Carotid blood flow and diameter were measured noninvasively by ultrasound biomicroscopy (Vevo 770; Visualsonic Inc.). Doppler incident angles were between 70° and 80°. A two-tailed student's *t* test, assuming equal variation, was performed to determine the significance of differences in carotid blood velocity.

1. Friedlander RM (2007) Clinical practice. Arteriovenous malformations of the brain. *N Engl J Med* 356:2704–2712.
2. Stapf C, *et al.* (2006) Invasive treatment of unruptured brain arteriovenous malformations is experimental therapy. *Curr Opin Neurol* 19:63–68.
3. Mullan S, Mojtahedi S, Johnson DL, Macdonald RL (1996) Embryological basis of some aspects of cerebral vascular fistulas and malformations. *J Neurosurg* 85:1–8.
4. Braverman IM, Keh A, Jacobson BS (1990) Ultrastructure and three-dimensional organization of the telangiectases of hereditary hemorrhagic telangiectasia. *J Invest Dermatol* 95:422–427.
5. Murray CD (1926) The physiological principle of minimum work: I. The vascular system and the cost of blood volume. *Proc Natl Acad Sci USA* 12:207–214.
6. Wang HU, Chen ZF, Anderson DJ (1998) Molecular distinction and angiogenic interaction between embryonic arteries and veins revealed by ephrin-B2 and its receptor Eph-B4. *Cell* 93:741–753.
7. Lai EC (2004) Notch signaling: Control of cell communication and cell fate. *Development* 131:965–973.
8. Villa N, *et al.* (2001) Vascular expression of Notch pathway receptors and ligands is restricted to arterial vessels. *Mech Dev* 108:161–164.
9. Lawson ND, Weinstein BM (2002) Arteries and veins: Making a difference with zebrafish. *Nat Rev Genet* 3:674–682.
10. Krebs LT, *et al.* (2004) Haploinsufficient lethality and formation of arteriovenous malformations in Notch pathway mutants. *Genes Dev* 18:2469–2473.
11. Carlson TR, *et al.* (2005) Endothelial expression of constitutively active Notch4 elicits reversible arteriovenous malformations in adult mice. *Proc Natl Acad Sci USA* 102:9884–9889.
12. Lawson ND, *et al.* (2001) Notch signaling is required for arterial-venous differentiation during embryonic vascular development. *Development* 128:3675–3683.
13. Uyttendaele H, Ho J, Rossant J, Kitajewski J (2001) Vascular patterning defects associated with expression of activated Notch4 in embryonic endothelium. *Proc Natl Acad Sci USA* 98:5643–5648.
14. Zhang J, *et al.* (2005) Mapping postnatal mouse brain development with diffusion tensor microimaging. *NeuroImage* 26:1042–1051.
15. Redfern CH, *et al.* (1999) Conditional expression and signaling of a specifically designed Gi-coupled receptor in transgenic mice. *Nat Biotechnol* 17:165–169.
16. Capron L (1988) in *Vascular Diseases*, ed Vinken PJ (Elsevier, New York), pp 35–62.
17. (2001) Reporting terminology for brain arteriovenous malformation clinical and radiographic features for use in clinical trials. *Stroke* 32:1430–1442.
18. Hellstrom M, *et al.* (2007) Dll4 signaling through Notch1 regulates formation of tip cells during angiogenesis. *Nature* 445:776–780.
19. Marks MP, Pelc NJ, Ross MR, Enzmann DR (1992) Determination of cerebral blood flow with a phase-contrast cine MR imaging technique: Evaluation of normal subjects and patients with arteriovenous malformations. *Radiology* 182:467–476.
20. Davy A, Soriano P (2007) Ephrin-B2 forward signaling regulates somite patterning and neural crest cell development. *Dev Biol* 304:182–193.
21. Scremin OU (1995) in *The Rat Nervous System*, ed Paxinos G (Academic, San Diego), pp 3–35.
22. Abdalla SA, Letarte M (2006) Hereditary haemorrhagic telangiectasia: Current views on genetics and mechanisms of disease. *J Med Genet* 43:97–110.
23. Matsubara S, *et al.* (2000) Angiographic and clinical characteristics of patients with cerebral arteriovenous malformations associated with hereditary hemorrhagic telangiectasia. *Am J Neuroradiol* 21:1016–1020.
24. Ogilvy CS, *et al.* (2001) Recommendations for the management of intracranial arteriovenous malformations: A statement for healthcare professionals from a special writing group of the Stroke Council, American Stroke Association. *Circulation* 103:2644–2657.
25. Anbarasu A, Gould DA (2002) Diagnosis of an intracranial arteriovenous malformation using extracranial carotid Doppler sonography. *J Clin Ultrasound* 30:249–252.
26. Fleetwood IG, Steinberg GK (2002) Arteriovenous malformations. *Lancet* 359:863–873.
27. Patel MC, Hodgson TJ, Kemeny AA, Forster DM (2001) Spontaneous obliteration of pial arteriovenous malformations: A review of 27 cases. *Am J Neuroradiol* 22:531–536.
28. Manning MW, Cassis LA, Daugherty A (2003) Differential effects of doxycycline, a broad-spectrum matrix metalloproteinase inhibitor, on angiotensin II-induced atherosclerosis and abdominal aortic aneurysms. *Arterioscler Thromb Vasc Biol* 23:483–488.
29. Lee CZ, *et al.* (2004) Doxycycline suppresses cerebral matrix metalloproteinase-9 and angiogenesis induced by focal hyperstimulation of vascular endothelial growth factor in a mouse model. *Stroke* 35:1715–1719.
30. Lee CZ, *et al.* (2007) Matrix metalloproteinase-9 inhibition attenuates vascular endothelial growth factor-induced intracerebral hemorrhage. *Stroke* 38:2563–2568.
31. Felsher DW, Bishop JM (1999) Reversible tumorigenesis by MYC in hematopoietic lineages. *Mol Cell* 4:199–207.
32. Wang R, *et al.* (2001) Activation of the Met receptor by cell attachment induces and sustains hepatocellular carcinomas in transgenic mice. *J Cell Biol* 153:1023–1034.
33. Weinstein IB (2002) Cancer. Addiction to oncogenes—the Achilles heal of cancer. *Science* 297:63–64.
34. Young WL, Yang GY (2004) Are there genetic influences on sporadic brain arteriovenous malformations? *Stroke* 35:2740–2745.
35. Maher CO, *et al.* (2001) Cerebrovascular manifestations in 321 cases of hereditary hemorrhagic telangiectasia. *Stroke* 32:877–882.
36. Bourdeau A, *et al.* (2001) Potential role of modifier genes influencing transforming growth factor-beta1 levels in the development of vascular defects in endoglin heterozygous mice with hereditary hemorrhagic telangiectasia. *Am J Pathol* 158:2011–2020.
37. Satomi J, *et al.* (2003) Cerebral vascular abnormalities in a murine model of hereditary hemorrhagic telangiectasia. *Stroke* 34:783–789.
38. Srinivasan S, *et al.* (2003) A mouse model for hereditary hemorrhagic telangiectasia (HHT) type 2. *Hum Mol Genet* 12:473–482.
39. Winick M (1976) in *Malnutrition and Brain Development*, ed Winick M (Oxford Univ Press, New York), pp 35–62.
40. Li JL, *et al.* (2007) Delta-like 4 Notch ligand regulates tumor angiogenesis, improves tumor vascular function, and promotes tumor growth in vivo. *Cancer Res* 67:11244–11253.
41. Ruhrberg C, *et al.* (2002) Spatially restricted patterning cues provided by heparin-binding VEGF-A control blood vessel branching morphogenesis. *Genes Dev* 16:2684–2698.
42. Carpenter B, *et al.* (2005) VEGF is crucial for the hepatic vascular development required for lipoprotein uptake. *Development* 132:3293–3303.
43. Braren R, *et al.* (2006) Endothelial FAK is essential for vascular network stability, cell survival, and lamellipodial formation. *J Cell Biol* 172:151–162.
44. Carlson TR, *et al.* (2008) Cell-autonomous requirement for {beta}1 integrin in endothelial cell adhesion, migration and survival during angiogenesis in mice. *Development* 135:2193–2202.